

Duration- and fetch-limited growth functions of wind-generated waves parameterized with three different scaling wind velocities

Paul A. Hwang^{1,2}

Received 20 July 2005; revised 7 November 2005; accepted 22 December 2005; published 11 February 2006.

[1] Under steady wind forcing, wave development follows the duration- and fetch-limited growth laws. These growth functions are used extensively to obtain the sea state information when only limited observations of the environmental variables are available. Validation and verification of wave models also employ numerical experiments of duration- and fetch-limited wave growth as benchmark tests. The reference wind speed reported in most of the wave-growth data is the equivalent neutral wind speed at 10 m elevation, U_{10} . It is generally believed that a more suitable scaling wind speed is either the wind friction velocity, u_* , or the wind speed at an elevation proportional to the wavelength of the ocean surface fluctuation, $U_{\lambda/2}$. The connection among the growth functions using different velocity scales is the drag coefficient of the ocean surface. In this paper, the similarity relation of the drag coefficient based on wavelength scaling is applied to the conversion of the wave growth functions from U_{10} to $U_{\lambda/2}$ and u_* scaling. The results are in good agreement with field measurements that include direct u_* measurements. Comparisons with numerical model output are also described.

Citation: Hwang, P. A. (2006), Duration- and fetch-limited growth functions of wind-generated waves parameterized with three different scaling wind velocities, *J. Geophys. Res.*, *111*, C02005, doi:10.1029/2005JC003180.

1. Introduction

[2] Duration- and fetch-limited wave-growth functions are of fundamental interest in basic research and engineering applications. They quantify the wave evolution under various driving forces represented by the source terms of the action density conservation equation. Some of the source functions are still poorly resolved and one of the methods to gauge the performance of numerical wave models is to compare the model results with fetch- or duration-limited wave-growth functions [e.g., *Komen et al.*, 1984, 1994; *Janssen et al.*, 1994; *Janssen*, 2004]. In the study of ocean surface wind stress, the growth function expressed as the dimensionless dependence of wave variance on wave frequency is invoked to make comparison among different expressions of the drag coefficient or dynamic roughness [e.g., *Toba et al.*, 2001; *Jones and Toba*, 2001; *Hwang*, 2005b]. Wave growth data are usually reported with the neutral wind speed at 10 m elevation, U_{10} , serving as the scaling wind velocity. So far, there have been many different growth functions proposed. The discrepancies among the proposed functions are caused mainly by the stability conditions, the combination of field and laboratory data in some of the analyses (e.g., see reviews by *Kahma and Calhoun* [1992, 1994] and *Young* [1999]), the spatial vari-

ability of the wind field caused by the proximity of land [*Dobson et al.*, 1989; *Donelan et al.*, 1992], and the difference in wave development stages in individual data sets [*Hwang and Wang*, 2004]. After sorting out the stability conditions, excluding laboratory data from the analysis, and using the average wind speed between measuring stations as the scaling wind velocity, *Kahma and Calhoun* [1992, 1994] found that many of the discrepancies can be reconciled. Three sets of equations were presented for stable stratification, unstable stratification, and composite data set.

[3] During the course of growth function investigation, an interesting question was raised regarding the best scaling wind velocity. The adaptation of U_{10} as the reference wind speed is mainly based on practical considerations. The scaling laws call for “free-stream” velocity, U_∞ [e.g., *Schlichting*, 1968; *Kitaigorodskii*, 1973]. For the marine atmospheric boundary layer modified by the ocean surface waves, one expects that the dynamic influence of surface waves to decay exponentially away from the air-sea interface with the decay rate scaled by the characteristic wavelength of the surface fluctuation [e.g., *Miles*, 1957; *Phillips*, 1977]. It is logical to consider that the wind speed at an elevation equal to one-half of the characteristic wavelength, $U_{\lambda/2}$, to be a reasonable representation of U_∞ . Another good candidate for the reference wind speed is the wind friction velocity, u_* , which is the square root of the ratio between the surface wind stress and the air density. For neutral stratification, the connection among the three wind speeds, U_{10} , $U_{\lambda/2}$, and u_* , is the logarithmic wind profile

$$U_z = \frac{u_*}{\kappa} \ln \frac{z}{z_0}, \quad (1)$$

¹Oceanography Division, Naval Research Laboratory, Stennis Space Center, Mississippi, USA.

²Temporarily at Remote Sensing Division, Naval Research Laboratory, Washington, D. C.

where U_z is the wind speed at elevation z , z_0 the dynamic roughness of the ocean surface, and $\kappa = 0.4$ the von Kármán constant. Equation (1) can also be written as

$$C_z^{-0.5} = \frac{1}{\kappa} \ln \frac{z}{z_0}, \quad (2)$$

where $C_z = u_*^2/U_z^2$ represents the drag coefficient referenced to U_z . Conversion of the growth functions from scaling with U_{10} to scaling with other wind velocities depends on a reliable function of the drag coefficient of the ocean surface, C_{10} . *Kahma and Calkoen* [1994] tested two different representations of C_{10} to convert the growth functions from U_{10} to u_* scaling. They reached the conclusion that the case for u_* scaling has not been proved and that if u_* is not measured, the algorithm chosen to estimate it may itself be a source of considerable error.

[4] Based on the consideration that surface waves are the ocean surface roughness element, and that the dynamic influence of surface waves decays exponentially with distance from the air-water interface, *Hwang* [2004] processed the drag coefficient $C_{\lambda/2}$ referenced to $U_{\lambda/2}$. The result yields significant improvement in agreement among different data sets and a similarity relation of $C_{\lambda/2}$ dependence on the dimensionless frequency scaled with u_* was developed. Subsequently, the similarity property of $C_{\lambda/2}$ was extended to dependence on the dimensionless frequency scaled with U_{10} [*Hwang*, 2005a, 2005c]. In this paper, the wavelength scaling of drag coefficient is applied to the conversion of wave growth functions from U_{10} to $U_{\lambda/2}$ and u_* scaling. The analytical expressions relating the three sets of growth functions are described in section 2. The analysis indicates that in order to use the similarity relation of $C_{\lambda/2}$, the ratio between $U_{\lambda/2}$ and U_{10} (denoted as R_U) needs to be considered. A discussion of R_U is presented. Section 3 provides a quantitative comparison of several different expressions of the drag coefficient. Section 4 presents the wave growth functions based on U_{10} , $U_{\lambda/2}$, and u_* scaling. Data from several field measurements of fetch- and duration-limited wave growth studies and air-sea interaction experiments are compiled to compare with the present conversion results. Comparisons with other proposed u_* scaling functions as well as numerical models are also discussed in this section. A summary is given in section 5.

2. Dimensionless Wave Growth Functions

[5] Considering the characteristic parameters of the gravity wave field (wave height H_s , or the variance of surface displacement σ^2 , and peak wave frequency ω_p); wind field (a reference wind velocity U), fetch x , duration t , and the environment (water depth d , and gravity g), the following dimensionless parameters can be established

$$e' = \frac{\sigma^2 g^2}{U^4}, \omega' = \frac{U \omega_p}{g}, x' = \frac{gx}{U^2}, t' = \frac{gt}{U}, d' = \frac{gd}{U^2}, \quad (3)$$

where a prime on a variable denotes its dimensionless representation. In the following discussions when it is necessary to distinguish among normalizations with U_{10} , $U_{\lambda/2}$, and u_* , the dimensionless variables are differentiated by subscripts $\#$, $*$, and $**$, respectively; that is,

$e_{\#} = \sigma^2 g^2/U_{10}^4$, $e_* = \sigma^2 g^2/U_{\lambda/2}^4$, $e_{**} = \sigma^2 g^2/u_*^4$, and so on. The similarity relation of the wave parameters can be expressed as

$$e' = f_1(x', t', d'), \quad \omega' = f_2(x', t', d'). \quad (4)$$

[6] If the local water depth is sufficiently deep and the duration of wind sufficiently long, the fetch-limited growth of wind-generated waves can be expressed simply by

$$e' = f_1(x'), \quad \omega' = f_2(x'). \quad (5)$$

Extensive efforts have been devoted to the establishment of the fetch-limited growth functions f_1 and f_2 (e.g., reviews by *Kahma and Calkoen* [1992, 1994] and *Young* [1999]). These efforts led to the conclusion that f_1 and f_2 can be represented by a power-law function for a wide range of the dimensionless fetch, approximately $10^2 < x_{\#} < 10^4$,

$$e_{\#} = Ax_{\#}^a, \quad \omega_{\#} = Bx_{\#}^b. \quad (6)$$

A summary of the coefficients A , a , B , and b from several different proposed functions is given in Appendix A. For $x_{\#} > 10^4$, the rate of wave development obviously slows down and (6) overestimates the dimensionless wave variance or wave period. *Donelan et al.* [1992] developed a differential expression of wave growth and produced analytical solutions of the growth functions in terms of $x_{\#}(\omega_{\#})$ and $x_{\#}(e_{\#})$,

$$x_{\#} = 4.0946 \times 10^4 \ln \left(\frac{1}{1 - 5.5414e_{\#}^{1/3.2}} \right) - 2.2690 \times 10^5 \left(1 + 2.7707e_{\#}^{1/3.2} \right) e_{\#}^{1/3.2}, \quad (7a)$$

$$x_{\#} = 4.0946 \times 10^4 \ln \left(\frac{\omega_{\#}}{\omega_{\#} - 0.8302} \right) - 3.3992 \times 10^4 (\omega_{\#} + 0.4151) \omega_{\#}^2. \quad (7b)$$

As commented by *Young* [1999], the transcendental nature of equations (7a) and (7b) makes solving $e_{\#}$ and $\omega_{\#}$ for given $x_{\#}$ a cumbersome process. *Hwang and Wang* [2004] developed a higher-order data-fitting technique to represent wave growth in the conventional power-law functions (equation (6)) but with the wave development rate varying with the dimensionless fetch, duration, or wave frequency. The procedure was applied to five different field data sets obtained in steady wind conditions [*Burling*, 1959; *Hasselmann et al.*, 1973; *Donelan et al.*, 1985; *Dobson et al.*, 1989; *Babanin and Soloviev*, 1998] (hereafter referred to as the BHDDDB data set; further description of the data set is given by *Hwang and Wang* [2004] and in Appendix A). The coefficients for the first- and second-order fitted growth functions are listed in Appendix A (equations (A12) and (A13)). With the power-law representation, it becomes much easier to transform the growth functions into different dependent variables. For example, *Hwang and Wang* [2004] converted the fetch-limited growth functions into duration-limited growth functions

$$e_{\#} = Pt_{\#}^p, \quad \omega_{\#} = Qt_{\#}^q. \quad (8)$$

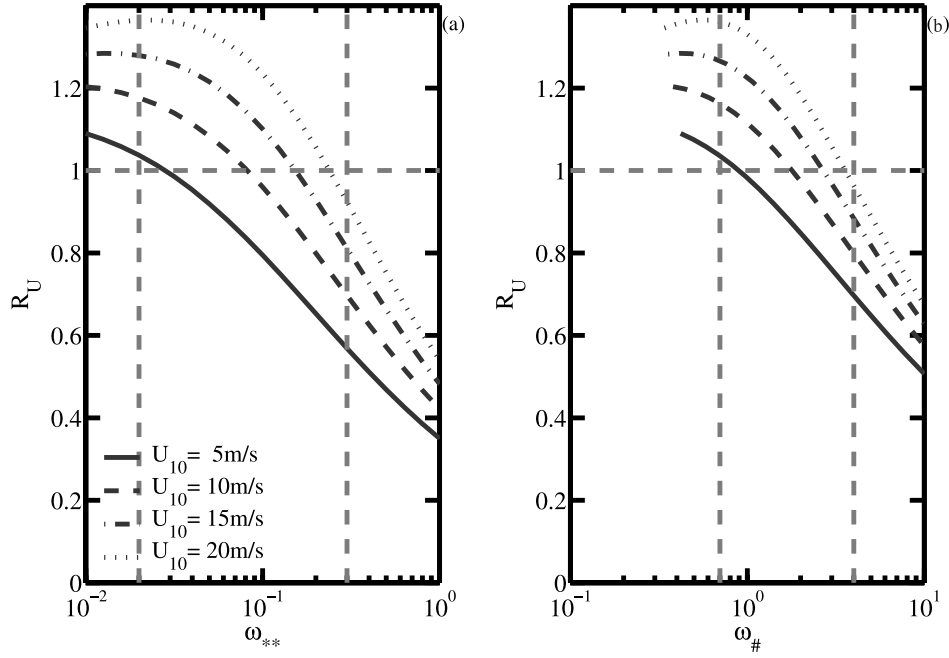


Figure 1. The velocity ratio $R_U = U_{\lambda/2}/U_{10}$, plotted as a function of (a) ω_{**} , and (b) $\omega_{\#}$ for several different wind speeds. The majority of reported ω_{**} and $\omega_{\#}$ falls between the two vertical dashed curves.

The coefficients P , p , Q , and q are simple algebraic functions of A , a , B , and b ,

$$P = A \left[\frac{R_c(b+1)}{B} \right]^{\frac{a}{b+1}}, \quad p = \frac{a}{b+1}, \quad (9)$$

$$Q = \left[\frac{1}{BbR_c(b+1)} \right]^{\frac{b}{b+1}}, \quad q = \frac{b}{b+1}$$

where $R_c \approx 0.4$ [Yefimov and Babanin, 1991] is the ratio between the effective group and phase velocities of the wave component at the spectral peak. The converted duration-limited growth functions compare very well with the limited amount of data on duration-limited wave growth collected from the ocean (see Figure 5 of Hwang and Wang [2004]). Because reliable duration-limited growth data are difficult to acquire from the field, making use of fetch-limited growth data to study the temporal growth of surface waves is very useful.

[7] When the reference wind speed is changed from U_{10} to $U_{\lambda/2}$ or u_* , the dimensionless parameters are related to each other by the drag coefficient, C_{10} or $C_{\lambda/2}$ [e.g., Komen *et al.*, 1994]

$$e_{**} = C_{10}^{-2} e_{\#}, \quad \omega_{**} = C_{10}^{0.5} \omega_{\#}, \quad x_{**} = C_{10}^{-1} x_{\#}, \quad t_{**} = C_{10}^{-0.5} t_{\#}$$

$$e_{**} = C_{\lambda/2}^{-2} e_*, \quad \omega_{**} = C_{\lambda/2}^{0.5} \omega_*, \quad x_{**} = C_{\lambda/2}^{-1} x_*, \quad t_{**} = C_{\lambda/2}^{-0.5} t_* \quad (10)$$

Substituting equation (10) to (6), the growth functions in terms of u_* are

$$e_{**} = C_{10}^{a-2} A x_{**}^a, \quad \omega_{**} = C_{10}^{b+0.5} B x_{**}^b. \quad (11)$$

The duration-limited growth functions in terms of u_* can be derived from equation (11) in a similar procedure as that of deriving equation (8) from equation (6).

[8] It is difficult to obtain a consistent parameterization of the ocean surface drag coefficient in terms of C_{10} . Hwang [2004, 2005a, 2005b, 2005c] showed that the similarity relation of ocean surface drag coefficient exists in wavelength scaling, $C_{\lambda/2}$. To make use of the $C_{\lambda/2}$ similarity to convert U_{10} scaling to u_* scaling of the wave growth functions, the following equalities can be used

$$e_* = R_U^{-4} e_{\#}, \quad \omega_* = R_U \omega_{\#}, \quad x_* = R_U^{-2} x_{\#}, \quad t_* = R_U^{-1} t_{\#}, \quad (12)$$

where

$$R_U = \frac{U_{\lambda/2}}{U_{10}} = \frac{\ln \pi - \ln(k_p z_0)}{\ln \left(\frac{\omega_{**}^2 g_{10}}{C_{\lambda/2} k_p z_0 U_{10}^2} \right) - 2 \ln(R_U)}, \quad (13)$$

and k_p is the wavenumber of the spectral peak component. The dimensionless roughness is related to $C_{\lambda/2}$ by the logarithmic wind profile, equation (2),

$$k_p z_0 = \pi \exp \left(-\kappa C_{\lambda/2}^{-0.5} \right). \quad (14)$$

R_U can be solved iteratively for given ω_{**} and U_{10} . From numerical experiment, with the initial guess of $R_{U0} = 1$, a relative error of 1 percent is achieved within five iterations [Hwang, 2005c]. Combining equations (6), (10), and (13), then

$$e_{**} = C_{\lambda/2}^{a-2} R_U^{2a-4} A x_{**}^a, \quad \omega_{**} = C_{\lambda/2}^{b+0.5} R_U^{2b+1} B x_{**}^b \quad (15)$$

Again, derivation of the duration-limited growth function from equation (15) is similar to that of deriving equation (8) from equation (6).

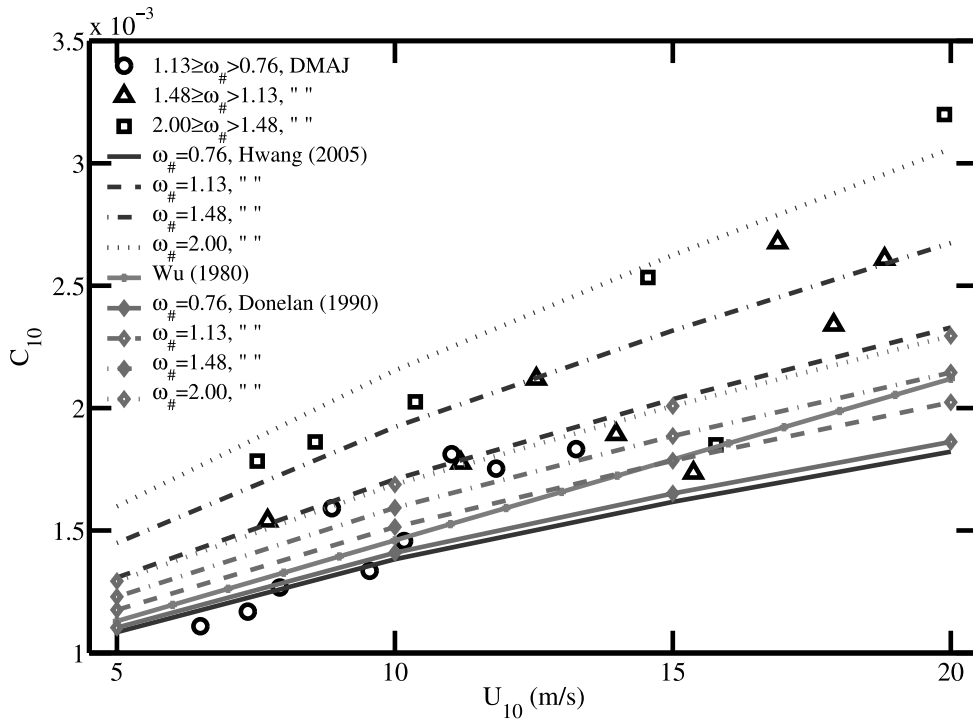


Figure 2. C_{10} calculated using the similarity relation of $C_{\lambda/2}$ from wavelength scaling [Hwang, 2005c]. The DMAJ data are superimposed for comparison.

[9] Equation (15) indicates that two factors, $C_{\lambda/2}$ and R_U , are needed to convert the growth functions from U_{10} to u_* scaling. Presently, the effort of conversion focuses on equation (11), however, the uncertainty in C_{10} parameterization has limited the progress. The issue of the parameterization of ocean surface drag coefficient has been extensively discussed in the literature and a brief review is given in section 3. In section 4, the conversion using equation (15) will be discussed. Here the factor R_U is examined. Figure 1 plots R_U as a function of ω_{**} and $\omega_{\#}$ with U_{10} as a parameter. Deviation of R_U from unity is a source of error in converting wave growth functions from U_{10} to u_* or $U_{\lambda/2}$ scaling. As shown in Figure 1, R_U varies with dimensionless frequency and wind speed in a systematic but complex fashion. Interestingly, as waves become more well-developed, R_U approaches asymptotically to a value about 1.10 for $U_{10} = 5$ m/s and about 1.35 for $U_{10} = 20$ m/s, with a mean value close to 1.25 over the whole range of wind speeds used in the computation. Empirically, it has been suggested that at full development, the phase speed of the wave component at the spectral peak, c_p , travels faster than the reference wind speed, U_{10} , with $c_p/U_{10} \approx 1.25$ [Pierson and Moskowitz, 1964]. Using $U_{\lambda/2}$ as the reference wind speed, the ratio $c_p/U_{\lambda/2}$ would have been close to unity. This provides an independent support for $U_{\lambda/2}$ serving as the free-stream velocity, U_{∞} .

3. Drag Coefficient of Wind-Generated Seas

[10] Kahma and Calkoen [1992, 1994] tested two different representations of C_{10} to convert the growth functions from U_{10} scaling to u_* scaling. The first one is a modified

Wu [1980] formula expressing C_{10} as a linear function of U_{10} ,

$$C_{10} = 8 \times 10^{-4} + 6.5 \times 10^{-5} \times \max\{U_{10}, 7.5\text{m/s}\}. \quad (16)$$

The second one is a wave-dependent z_0 proposed by Donelan [1990],

$$\frac{z_0}{\sigma} = 5.53 \times 10^{-4} \left(\frac{U_{10}}{c_p} \right)^{2.66}. \quad (17)$$

Figure 2 compares the drag coefficient computed from equations (16) and (17) with the results obtained from direct wind stress measurements in the field under fetch-limited wave conditions. The field data set represents the combined results of four different experiments [Donelan, 1979; Merzi and Graf, 1985; Anctil and Donelan, 1996; Janssen, 1997] (hereafter referred to as the DMAJ data set; the experimental conditions were summarized by Hwang [2004]), that covers a wide range of the wave development condition, $0.0235 < \omega_p u_* / g < 0.237$ and $0.0263 < u_* / c_p < 0.237$. As shown in Figure 2, the Wu [1980] expression of C_{10} is only suitable for describing the ocean surface drag condition at more mature sea state (for $\omega_{\#}$ in the neighborhood of unity). C_{10} computed from Donelan [1990] roughness expression, equation (17), shows dependence on both U_{10} and $\omega_{\#}$ but the range of variation on $\omega_{\#}$ is smaller than that observed in the field data by about a factor-of-two (Figure 2). Hwang [2004, 2005a, 2005b, 2005c] suggested that the difficulty in finding the similarity properties of the ocean-surface drag coefficient can be attributed to the choice of the arbitrary 10-m as the length scale for wind-speed reference. When

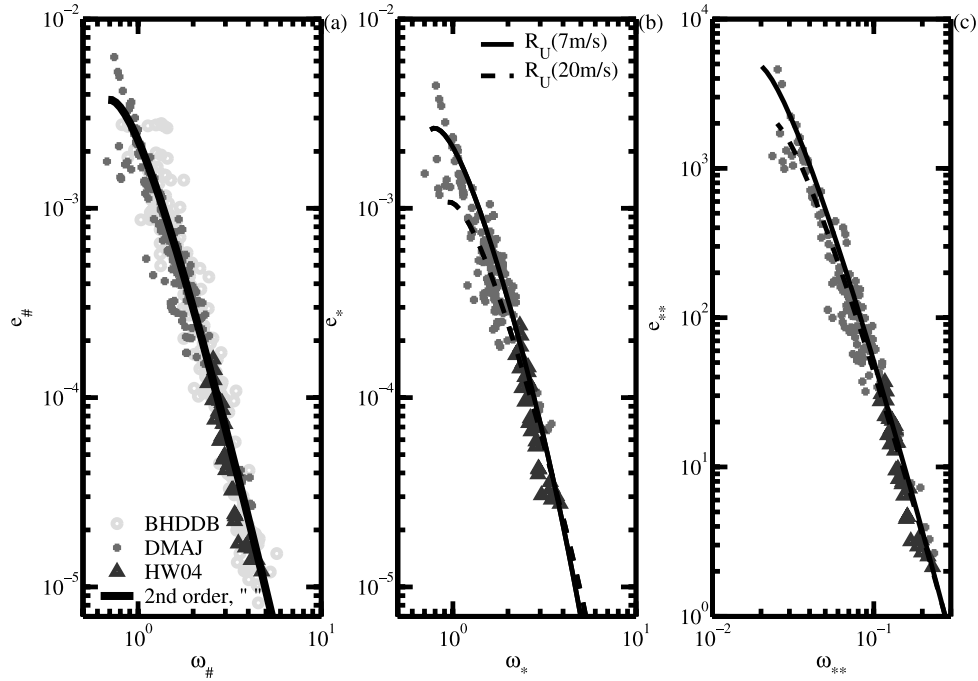


Figure 3. Fetch- and duration-limited wave growth data represented as $e'(\omega')$ with (a) U_{10} , (b) $U_{\lambda/2}$, and (c) u_* scaling.

processed with wavelength scaling, a strong similarity behavior exists in wind-stress measurements represented either by the drag coefficient or the dynamic roughness,

$$C_{\lambda/2} = A_c \left(\frac{\omega_p u_*}{g} \right)^{a_c}, \text{ with } A_c = 1.220 \times 10^{-2} \text{ and } a_c = 0.704. \quad (18)$$

Using equation (18), the dimensionless roughness expressed as $k_p z_0$ can be easily computed with the application of the logarithmic wind speed profile (equation (14)). The dimensionless roughness can also be expressed as z_0/σ with the additional application of the fetch-limited growth function, $e_{\#}(\omega_{\#})$. Furthermore, $C_{10}(U_{10}, \omega_{\#}) = C_{\lambda/2} R_U^2$ can be derived from equations (18) and (13) [Hwang, 2005c]. The result is in good agreement with field observations (Figure 2). For practical applications, the following parameterization function is developed from the DMAJ data set [Hwang, 2005a, 2005c]

$$C_{\lambda/2} = A_{10} \left(\frac{\omega_p U_{10}}{g} \right)^{a_{10}}, \text{ with } A_{10} = 1.289 \times 10^{-3} \text{ and } a_{10} = 0.815. \quad (19)$$

4. Comparison with Field Data and Model Results

[11] Most experiments on fetch-limited wave growth studies, such as BHDDB, do not report direct wind stress measurements so they cannot provide an unambiguous assessment on the growth functions using different scaling wind velocities. Direct wind stress measurements are usu-

ally performed in air-sea interaction experiments, especially for the parameterization of ocean surface drag coefficient. The DMAJ data set was obtained under fetch-limited growth conditions with sufficient details reported to facilitate the computation of $U_{\lambda/2}$. Figure 3 shows the comparison of these two large data sets. Because many of the experiments on air-sea interaction do not report wind fetch, the comparison is shown in $e'(\omega')$. In addition to the two combined fetch-limited data sets, measurements from a recent duration-limited wave growth study [Hwang and Wang, 2004] are also superimposed. Considering the disparate conditions under which these data were collected, the varieties of instruments used, and the differences in processing procedures by different research groups, the general agreement of the results shown in Figure 3a is impressive. The curve plotted in the panel used for visual reference is equation (A13), which is derived from the second-order fitting procedure applied to the BHDDB data set [Hwang and Wang, 2004]. In Figures 3b and 3c, equation (15) is used to convert the wave growth functions from U_{10} to $U_{\lambda/2}$ and u_* scaling. As mentioned earlier, to use equation (15), $C_{\lambda/2}$ and R_U need to be calculated. For the DMAJ data set, direct measurements of u_* and k_p were reported and the computation of $C_{\lambda/2}$ and R_U is straightforward [Hwang, 2004, 2005c]. For the duration-limited data set of Hwang and Wang [2004], k_p is available, but the fast evolution of the wave field requires high temporal resolution, on the order of 164-s duration for each wave spectral computation. Such duration is too short for reliable wind stress processing and bulk formulae are used to obtain u_* . Here u_* computed by equation (19) is chosen. More details on u_* computation using bulk formulae are given in Appendix B. For the BHDDB data set (digitized from dimensionless plots of $e_{\#}(x_{\#})$ or $e_{\#}(\omega_{\#})$ and $\omega_{\#}(x_{\#})$ in the original papers), simulta-

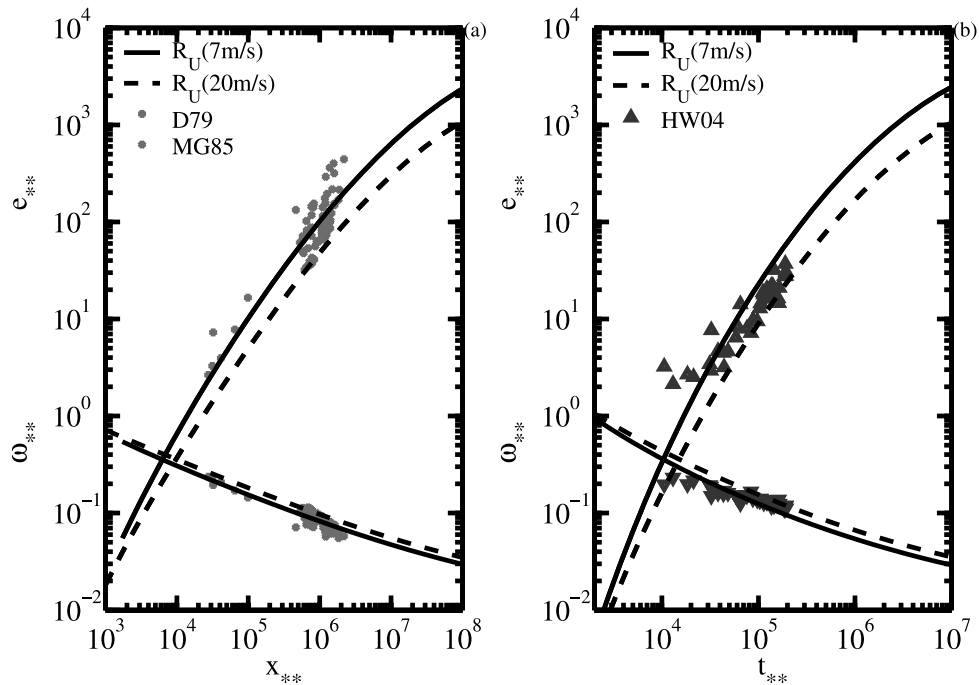


Figure 4. (a) Fetch-, and (b) duration-limited growth functions in u_* scaling, and comparison with available field data.

neous $\omega_{\#}$ and U_{10} are not available to compute R_U (Figure 1). The curves corresponding to $U_{10} = 7$ and 20 m/s are applied to equation (A13) to represent the possible range of the average of the BHDDB data set. The growth functions scaling with $U_{\sqrt{2}}$ and u_* and converted from those with U_{10} scaling are in very good agreement with the results based on

the DMAJ data set with direct u_* measurements, and the Hwang and Wang [2004] data set with u_* calculated by equation (19).

[12] The growth functions $e_{**}(x_{**})$, $\omega_{**}(x_{**})$, $e_{**}(t_{**})$, and $\omega_{**}(t_{**})$ are shown in Figure 4. A subset of the DMAJ data set, Donelan [1979] and Merzi and Graf [1985], listed

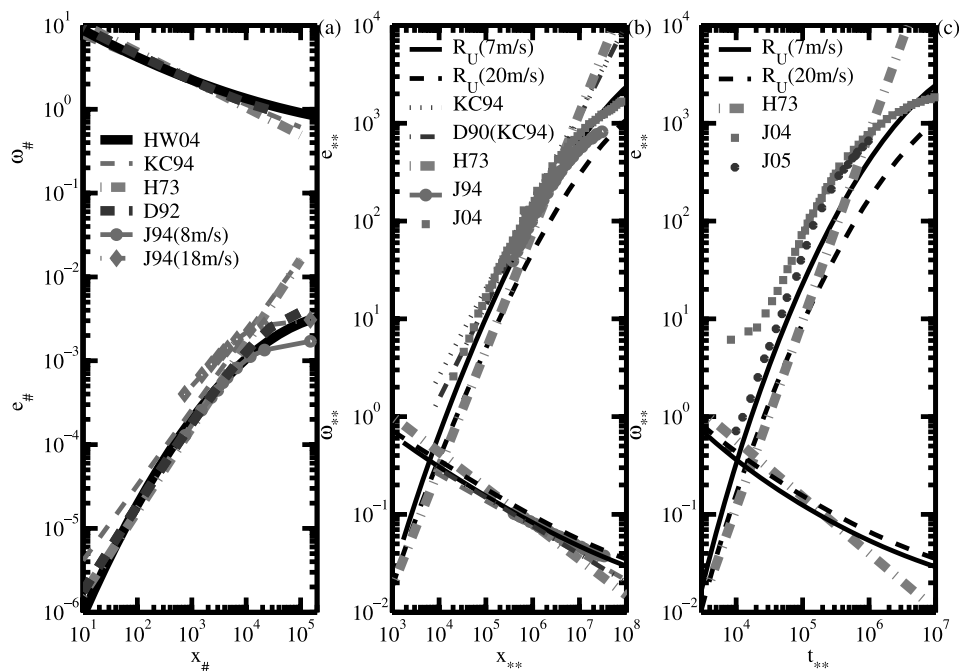


Figure 5. Comparison of the wave growth functions with several other different expressions and numerical model results. (a) U_{10} scaling, fetch-limited growth; (b) u_* scaling, fetch-limited growth; and (c) u_* scaling, duration-limited growth.

wind fetch so they can be compared with the analytical computation of the fetch-limited wave growth functions (Figure 4a). The duration-limited measurements of *Hwang and Wang* [2004] are shown in Figure 4b to compare with the analytical computation of the duration-limited wave growth functions. The agreement appears to be very good considering the large data scatter in the measurements.

[13] Figure 5 presents the wave growth functions scaled by U_{10} and u_* . In panel (a), several proposed growth functions of $e_{\#}(x_{\#})$ and $\omega_{\#}(x_{\#})$, as summarized in Appendix A, are plotted together [Hasselmann *et al.*, 1973; Donelan *et al.*, 1992; Kahma and Calkoen, 1994; Hwang and Wang, 2004]. In general, all different expressions of the growth functions show very good agreement in the middle range of the dimensionless fetch about $x_{\#} = 10^3$. Deviation of the simple power-law growth functions from observations is found at earlier and later stages of wave development. The slowing down of wave growth as dimensionless fetch increases is reproduced reasonably well by numerical wave models [e.g., Janssen *et al.*, 1994; Janssen, 2004]. The disadvantage of using U_{10} as the scaling wind speed is demonstrated clearly in numerical experiments. An example is given in Figure 3.22 of Janssen *et al.* [1994], which is reproduced in Figure 5a, showing that the computed dimensionless function $\omega_{\#}(x_{\#})$ displays additional dependence on the wind speed. Scaling with u_* is considered to be a solution to the problem associated with U_{10} scaling. Because the uncertainty in finding a suitable C_{10} parameterization, it remains a difficult task establishing growth functions using u_* scaling. The results reported by Kahma and Calkoen [1994], as described in section 3, are shown in Figure 5b. Also plotted in this panel are the numerical model results reported by Janssen *et al.* [1994, Figures 3.25 and 3.26] and Janssen [2004, Figure 5.10] and the conversion using the $C_{\lambda/2}$ similarity relation described in section 2. Figure 5c shows the result on duration-limited growth functions. The numerical results of duration-limited growth given by Janssen [2004, Figure 5.7] are superimposed. Discrepancies between numerical simulations and the empirical functions of the present analysis can be attributed to several factors. First, differences in the data sets used for constructing the growth functions that the wave model was tuned to. Second, the drag coefficient used in converting from U_{10} to u_* scaling; more detail discussion of the issue is given in Appendix B. Briefly, e_{**} is proportional to u_*^{-4} , which in turn is proportional to C_z^{-2} . Therefore, a factor-of-two underestimation of C_z (not uncommon for young wave fields, see Appendix B) would overestimate e_{**} by a factor-of-four. This is not only a problem for duration-limited growth study, it also occurs in fetch-limited growth, as illustrated by the large difference between the two numerical model curves computed for 8 and 18 m/s winds [Janssen *et al.*, 1994] shown in Figure 5a. Third, the incorporation of R_U in the conversion method also plays a minor role. A fourth factor contributing to the discrepancy between observed and modeled duration-limited growth curves is the initial condition (of peak spectral frequency at 0.34 Hz) and the resolved frequency range (maximum frequency 0.7 Hz) of model runs used in Janssen [2004]. Janssen (personal communication, 2005) performed the same numerical experiment of duration-limited growth with a higher initial peak frequency (0.9 Hz) and the frequency

range of computation expanded to 2 Hz. The trend of the wave growth (shown as circles in Figure 5c) is in much better agreement with the empirical curve derived from the present analysis.

[14] Because fetch- and duration-limited growth data with u_* measurements are rare, conversion of $e_{\#}(x_{\#})$ and $\omega_{\#}(x_{\#})$ to $e_{**}(x_{**})$, $\omega_{**}(x_{**})$, $e_{**}(t_{**})$, and $\omega_{**}(t_{**})$ remains a necessary task to enlarge the field database for model validation and verification. The method described in this paper makes use of the similarity relation of the drag coefficient based on wavelength scaling and considers the factor $U_{\lambda/2}/U_{10}$.

5. Summary

[15] While U_{10} is used extensively as the reference wind speed in the research of wind-wave growth and air-sea interaction, the choice of 10-m as the reference elevation of wind speed measurement is mainly due to practical consideration rather than the dynamic significance of the 10-m elevation in the marine boundary layer. Searching for an alternative scaling velocity has been a continuous effort over the last few decades. It is believed that either $U_{\lambda/2}$ or u_* is more preferable than U_{10} to serve as the scaling wind speed. The former is a reasonable substitute for the free-stream velocity used in the dimensionless analysis of wave growth functions (section 2), and the latter represents the wind stress applied at the ocean surface. Converting from U_{10} to $U_{\lambda/2}$ or u_* scaling requires an accurate prescription of the drag coefficient of the ocean surface. Although there have been many formulae proposed for C_{10} , it is difficult to express its complex dependence on U_{10} and $\omega_{\#}$ in an analytical form amenable to computation. Recently, Hwang [2004, 2005a, 2005b, 2005c] showed that the parameterization of ocean surface drag coefficient simplifies considerably when $U_{\lambda/2}$ is used as the velocity scale, and similarity relation exists in both the drag coefficient and the dynamic roughness. The similarity relation of the drag coefficient based on wavelength scaling is used in this paper to convert the wave growth functions from U_{10} to $U_{\lambda/2}$ and u_* scaling. The results are in good agreement with the limited field data that provide u_* measurements and fetch or duration information to form dimensionless parameters scaled with u_* .

Appendix A: A Summary of the Fetch-Limited Growth Functions

[16] The following fetch-limited growth functions are mostly compiled by Kahma and Calkoen [1994] and Young [1999].

[17] Sverdrup, Munk and Bretschneider empirical functions (SMB) [CERC, 1977]

$$e_{\#} = 5.0 \times 10^{-3} \tanh^2 \left(0.0125 x_{\#}^{0.42} \right), \omega_{\#} = \frac{0.835}{\tanh \left(0.077 x_{\#}^{0.25} \right)}. \quad (\text{A1})$$

(Note: combined laboratory and field data sources.)

[18] Pierson-Moskowitz limit of fully-developed seas [Pierson and Moskowitz, 1964]

$$e_{\#} = 3.64 \times 10^{-3}, \omega_{\#} = 0.82. \quad (\text{A2})$$

Table A1. Coefficients of the Fetch-Growth Similarity Laws

		$e_{\#} = A x_{\#}^a$ and $\omega_{\#} = B x_{\#}^b$			
Source		A	a	B	b
1.	SMB [CERC, 1977] ^a	7.82×10^{-7}	0.84	10.82	-0.25
2.	JONSWAP [Hasselmann <i>et al.</i> , 1973] ^a	1.60×10^{-7}	1.00	21.98	-0.33
3.	Bothnian Sea (unstable) [Kahma, 1981]	3.60×10^{-7}	1.00	19.97	-0.33
4.	Lake Ontario [Donelan <i>et al.</i> , 1985]	8.42×10^{-7}	0.76	11.62	-0.23
5.	North Atlantic [Dobson <i>et al.</i> , 1989]	1.27×10^{-6}	0.75	10.68	-0.24
6.	Lake St. Clair [Donelan <i>et al.</i> , 1992] ^b	2.60×10^{-7}	0.95	17.59	-0.30
7.	Composite stable [Kahma and Calkoen, 1994]	9.30×10^{-7}	0.77	12.00	-0.24
8.	Composite unstable [Kahma and Calkoen, 1994]	5.40×10^{-7}	0.94	14.00	-0.28
9.	Composite mixed [Kahma and Calkoen, 1994]	5.20×10^{-7}	0.90	13.70	-0.27
10.	Average [Young, 1999]	7.50×10^{-7}	0.80	12.56	-0.25
11.	Fetch-dependent growth rate (equations (A12) and (A13)) [Hwang and Wang, 2004]	6.19×10^{-7}	0.81	11.86	-0.24

^aSMB and JONSWAP combine field and laboratory data.

^bThe asymptotic form of the original implicit functions of dimensionless energy and frequency for the range $100 < x_{\#} < 3000$.

[19] JONSWAP fetch-limited wave evolution [Hasselmann *et al.*, 1973]

$$e_{\#} = 1.6 \times 10^{-7} x_{\#}, \quad \omega_{\#} = 21.98 x_{\#}^{-0.33}. \quad (\text{A3})$$

(Note: combined laboratory and field data sources.)

[20] Bothnian Sea [Kahma, 1981]

$$e_{\#} = 3.60 \times 10^{-7} x_{\#}, \quad \omega_{\#} = 19.97 x_{\#}^{-0.33}. \quad (\text{A4})$$

(Note: strongly unstable conditions.)

[21] Lake Ontario [Donelan *et al.*, 1985]

$$e_{\#} = 2.74 \times 10^{-3} \omega_{\#}^{-3.3}, \quad \omega_{\#} = 11.6 x_{\#}^{-0.23}. \quad (\text{A5a, A5b})$$

Combining (A5a) and (A5b),

$$e_{\#} = 8.415 \times 10^{-7} x_{\#}^{0.76}. \quad (\text{A5c})$$

North Atlantic open ocean [Dobson *et al.*, 1989]

$$e_{\#} = 1.27 \times 10^{-6} x_{\#}^{0.75}, \quad \omega_{\#} = 10.68 x_{\#}^{-0.24}. \quad (\text{A6})$$

(Note: the analysis took into account the coastal effect on the wind field and used the integrated wind speed up-fetch as the scaling wind velocity.)

[22] Lake St. Clair [Donelan *et al.*, 1992]

$$x_{\#} = 4.0946 \times 10^4 \ln \left(\frac{1}{1 - 5.5414 e_{\#}^{1/3.2}} \right) - 2.269 \times 10^5 \left(1 + 2.7707 e_{\#}^{1/3.2} \right) e_{\#}^{1/3.2}, \quad (\text{A7a})$$

$$x_{\#} = 4.0946 \times 10^4 \ln \left(\frac{\omega_{\#}}{\omega_{\#} - 0.829} \right) - \frac{8.616 \times 10^{-4} (\omega_{\#} + 0.414)}{\omega_{\#}^2}. \quad (\text{A7b})$$

(Note: $e_{\#}$ and $\omega_{\#}$ are implicit functions of $x_{\#}$. The additional digits beyond second decimal place in (A7a) and (A7b) not available in the original paper, were supplied by M. Donelan (personal communication).)

[23] Composite field data [Kahma and Calkoen, 1992, 1994].

[24] The Bothnian Sea data set highlights the significant influence of the stability effect. Kahma and Calkoen [1992, 1994] suggested the following stability adjustment based on reanalysis of several field data sets.

[25] Stable stratification:

$$e_{\#} = 9.3 \times 10^{-7} x_{\#}^{0.77}, \quad \omega_{\#} = 12 x_{\#}^{-0.24}. \quad (\text{A8})$$

Unstable stratification:

$$e_{\#} = 5.4 \times 10^{-7} x_{\#}^{0.94}, \quad \omega_{\#} = 14 x_{\#}^{-0.28}. \quad (\text{A9})$$

Combined field data:

$$e_{\#} = 5.2 \times 10^{-7} x_{\#}^{0.9}, \quad \omega_{\#} = 13.7 x_{\#}^{-0.27}. \quad (\text{A10})$$

Average and bounds [Young, 1999]

$$e_{\#} = \max \left\{ \begin{array}{l} (7.5 \pm 2.0) \times 10^{-7} x_{\#}^{0.8} \\ (3.6 \pm 0.9) \times 10^{-3} \end{array} \right\}, \quad (\text{A11})$$

$$\omega_{\#} = \min \left\{ \begin{array}{l} (12.56 \pm 1.88) x_{\#}^{-0.25} \\ (0.82 \pm 0.13) \end{array} \right\}.$$

Fetch-dependent growth rate [Hwang and Wang, 2004].

[26] Hwang and Wang [2004] included the data sets reported by Burling [1959] and Babanin and Soloviev [1998] with other measurements (BHDDDB) to derive the fetch laws

$$e_{\#} = 6.1910 \times 10^{-7} x_{\#}^{0.8106}, \quad \omega_{\#} = 11.86 x_{\#}^{-0.2368}. \quad (\text{A12})$$

They also developed a higher-order fitting technique to describe wave growth in power-law functions with variable proportionality coefficient and exponent. To the second order,

$$e_{\#} = A_2 x_{\#}^{a_2}, \quad \omega_{\#} = B_2 x_{\#}^{b_2},$$

$$A_2 = \exp(\alpha_0) x_{\#}^{-\alpha_2 \ln x_{\#}}, \quad a_2 = \alpha_1 + 2\alpha_2 \ln x_{\#}, \quad (\text{A13})$$

$$B_2 = \exp(\beta_0) x_{\#}^{-\beta_2 \ln x_{\#}}, \quad b_2 = \beta_1 + 2\beta_2 \ln x_{\#},$$

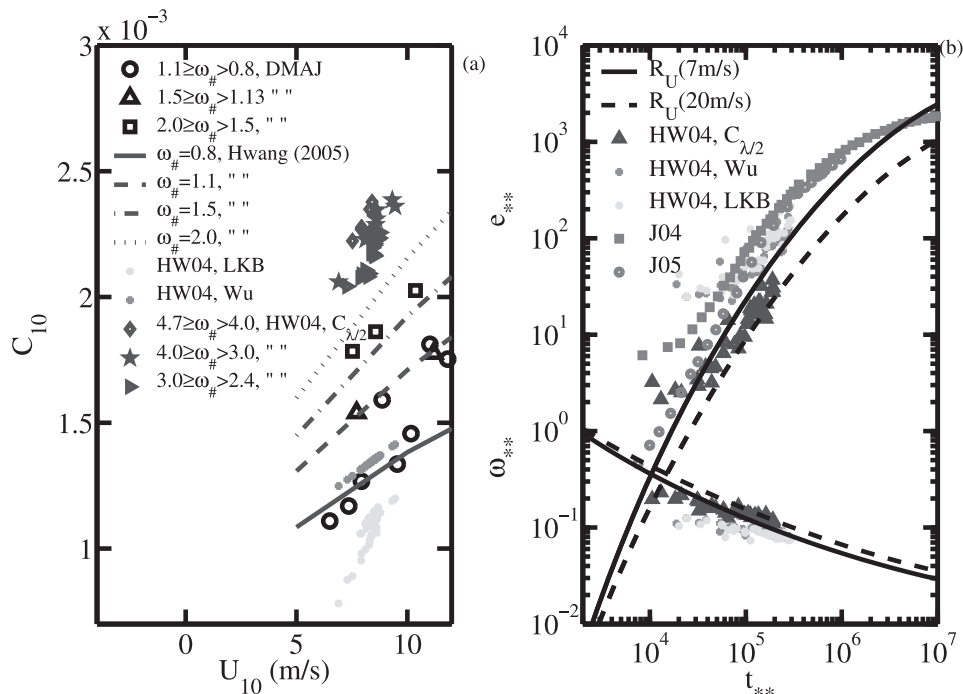


Figure B1. (a) C_{10} of Hwang and Wang [2004] data set calculated using the similarity relation of $C_{\lambda/2}$ (equation (19)), wind-dependent C_{10} [Wu, 1980], and the LKB bulk parameterization [Liu et al., 1979]. The DMAJ data are superimposed for comparison. (b) The impact on the growth curves by using different u_* .

with $\alpha_0 = 3.0377$, $\alpha_1 = -0.3990$, $\alpha_2 = 0.0110$, $\beta_0 = -17.6158$, $\beta_1 = 1.7645$, and $\beta_2 = -0.0647$. Table A1 presents a summary of A , a , B , and b of various growth functions described above.

Appendix B: Computation of u_* of Hwang and Wang [2004] Data Set

[27] The duration-limited wave growth data reported by Hwang and Wang [2004] were collected in the first two hours of wave development after the beginning of a steady wind event in a sheltered bay. Because the wave development is very fast at such an early stage, the duration of data segments for wave spectral processing is about 164 s. This duration is too short for reliable wind stress computation and parameterization equations need to be used to calculate u_* . Figure B1a shows the results obtained from the LKB bulk parameterization [Liu et al., 1979], wind-speed dependent C_{10} by Wu [1980], and $C_{\lambda/2}$ similarity function, equation (19). The trend of $C_{10}(U_{10}, \omega_{\#})$ derived from equation (19) is consistent with the results displayed by the direct wind stress measurements of the DMAJ data set. In contrast, the LKB and Wu parameterizations seem to be unsuitable for application to very young seas. Because e_{**} is proportional to u_*^{-4} and t_{**} is proportional to u_*^{-1} , when a lower u_* value is used in the scaling, the growth curve shifts upward and right-ward, but the upward shift is four times as much as the right-ward shift in log-log scales (Figure B1b). In Figure B1b, the numerical model results of $e_{**}(t_{**})$ reported by Janssen [2004, Figure 5.7] and the rerun (Janssen, personal communication, 2005) as described in the text are also shown.

[28] **Acknowledgments.** This work is sponsored by the Office of Naval Research (Naval Research Laboratory PE61153N and PE62435N). NRL contribution NRL/JA/7330-05-5293.

References

- Anctil, F., and M. A. Donelan (1996), Air-water momentum flux observed over shoaling waves, *J. Phys. Oceanogr.*, *26*, 1344–1353.
- Babanin, A. V., and Y. P. Soloviev (1998), Field investigation of transformation of the wind wave frequency spectrum with fetch and the stage of development, *J. Phys. Oceanogr.*, *28*, 563–576.
- Burling, R. W. (1959), The spectrum of waves at short fetches, *Dtsch. Hydrogr. Z.*, *12*, 96–117.
- CERC (1977), Shore Protection Manual, 3 vols., U.S. Army Coastal Eng. Res. Cent., Washington, D.C.
- Dobson, F., W. Perrie, and B. Toulany (1989), On the deep-water fetch laws for wind-generated surface gravity waves, *Atmos. Ocean*, *27*, 210–236.
- Donelan, M. A. (1979), On the fraction of wind momentum retained by waves, in *Marine Forecasting*, edited by J. C. J. Nihoul, pp. 141–159, Elsevier, New York.
- Donelan, M. A. (1990), Air-sea interaction, in *The Sea*, vol. 9, *Ocean Engineering Science*, edited by B. LeMehaute and D. M. Hanes, pp. 239–292, Wiley Interscience, Hoboken, N. J.
- Donelan, M. A., J. Hamilton, and W. H. Hui (1985), Directional spectra of wind-generated waves, *Philos. Trans. R. Soc. London, Ser. A*, *315*, 509–562.
- Donelan, M. A., M. Skafel, H. Graber, P. Liu, D. Schwab, and S. Venkatesh (1992), On the growth rate of wind-generated waves, *Atmos. Ocean*, *30*, 457–478.
- Hasselmann, K., et al. (1973), Measurements of wind-wave growth and swell decay during the Joint North Sea Wave Project (JONSWAP), *Dtsch. Hydrogr. Z.*, *12*(suppl. A), 95 pp.
- Hwang, P. A. (2004), Influence of wavelength on the parameterization of drag coefficient and surface roughness, *J. Oceanogr.*, *60*, 835–841.
- Hwang, P. A. (2005a), Comparison of the ocean surface wind stress computed with different parameterization functions of the drag coefficient, *J. Oceanogr.*, *61*, 91–107.
- Hwang, P. A. (2005b), Drag coefficient, dynamic roughness and reference wind speed, *J. Oceanogr.*, *61*, 399–413.
- Hwang, P. A. (2005c), Temporal and spatial variation of the drag coefficient of a developing sea under steady wind forcing, *J. Geophys. Res.*, *110*, C07024, doi:10.1029/2005JC002912.

- Hwang, P. A., and D. W. Wang (2004), Field measurements of duration-limited growth of wind-generated ocean surface waves at young stage of development, *J. Phys. Oceanogr.*, *34*, 2316–2326, (Corrigendum, *J. Phys. Oceanogr.* *35*, 268–270, 2005).
- Janssen, J. A. M. (1997), Does wind stress depend on sea-state or not?—A statistical error analysis of HEXMAX data, *Boundary Layer Meteorol.*, *83*, 479–503.
- Janssen, P. (2004), *The Interaction of Ocean Waves and Wind*, 300 pp., Cambridge Univ. Press, New York.
- Janssen, P. A. E. M., et al. (1994), Numerical modelling of wave evolution, in *Dynamics and Modeling of Ocean Waves*, edited by G. J. Komen et al., pp. 205–257, Cambridge Univ. Press, New York.
- Jones, I. S. F., and Y. Toba (Eds.) (2001), *Wind Stress Over the Ocean*, 307 pp., Cambridge Univ. Press, New York.
- Kahma, K. K. (1981), A study of the growth of the wave spectrum with fetch, *J. Phys. Oceanogr.*, *11*, 1503–1515.
- Kahma, K. K., and C. J. Calkoen (1992), Reconciling discrepancies in the observed growth of wind-generated waves, *J. Phys. Oceanogr.*, *22*, 1389–1405.
- Kahma, K. K., and C. J. Calkoen (1994), Growth curve observations, in *Dynamics and Modeling of Ocean Waves*, edited by G. J. Komen et al., pp. 174–182, Cambridge Univ. Press, New York.
- Kitaigorodskii, S. A. (1973), *The Physics of Air-Sea Interaction* (English translation), 237 pp., *Isr. Program for Sci. Transl.*, Jerusalem, Israel.
- Komen, G. J., K. Hasselmann, and S. Hasselmann (1984), On the existence of a fully developed wind-sea spectrum, *J. Phys. Oceanogr.*, *14*, 1271–1285.
- Komen, G. J., L. Cavaleri, M. Donelan, K. Hasselmann, S. Hasselmann, and P. A. E. M. Janssen (Eds.) (1994), *Dynamics and Modeling of Ocean Waves*, 532 pp., Cambridge Univ. Press, New York.
- Liu, W. T., K. B. Katsaros, and J. A. Businger (1979), Bulk parameterization of air-sea exchanges of heat and water-vapor including the molecular constraints at the interface, *J. Atmos. Sci.*, *36*, 1722–1735.
- Merzi, N., and W. H. Graf (1985), Evaluation of the drag coefficient considering the effects of mobility of the roughness elements, *Ann. Geophys.*, *3*, 473–478.
- Miles, J. W. (1957), On the generation of surface waves by shear flows, *J. Fluid Mech.*, *3*, 185–204.
- Phillips, O. M. (1977), *The Dynamics of the Upper Ocean*, 2nd ed., 366 pp., Cambridge Univ. Press, New York.
- Pierson, W. J., and L. Moskowitz (1964), A proposed spectral form for full, developed wind seas based on the similarity theory of S. A. Kitaigorodskii, *J. Geophys. Res.*, *69*, 5181–5190.
- Schlichting, H. (1968), *Boundary-Layer Theory*, translated by J. Kestin, 748 pp., McGraw-Hill, New York.
- Toba, Y., S. D. Smith, and N. Ebuchi (2001), Historical drag expressions, in *Wind Stress Over the Ocean*, edited by I. S. F. Jones and Y. Toba, pp. 35–53, Cambridge Univ. Press, New York.
- Wu, J. (1980), Wind-stress coefficients over sea surface near neutral conditions—A revisit, *J. Phys. Oceanogr.*, *10*, 727–740.
- Yefimov, V. V., and A. V. Babanin (1991), Dispersion relation for the envelope of groups of wind waves, *Izv. Atmos. Oceanic Phys.*, *27*, 599–603.
- Young, I. R. (1999), *Wind Generated Ocean Waves*, 288 pp., Elsevier, New York.

P. A. Hwang, Remote Sensing Division, Naval Research Laboratory, Bldg. 2, Room 244E, 4555 Overlook Avenue SW, Washington, DC 20375, USA. (phwang@ccs.nrl.navy.mil)